2008 IEEE International Conference on
Robotics and Automation
Pasadena, CA, USA, May 19-23, 2008

# A New Robust Stability Analysis and Design Tool for Bilateral Teleoperation Control Systems

Amir Haddadi and Keyvan Hashtrudi-Zaad, *member, IEEE*

***Abstract*— In this paper, a powerful robust stability analysis technique is introduced and developed for teleoperation systems. The methodology is based on wave parameters and discusses absolute stability and potential instability using scattering and is originally used in microwave systems [1]. The proposed method provides suitable mathematical and visual aids to determine bounds or regions of passive environment impedances for which a potentially unstable system connected to any passive operator is stable, and vice-versa. Furthermore, a novel stability parameter is proposed to maximize the derivation of the above bounds or regions. This results in less conservative guaranteed stability conditions compared to the Llewellyn's criterion; thus, achieving a better compromise between stability and performance. The proposed methodology allows for the design of bilateral control systems when such bounds are known or even when the operator or environment dynamics are active. The new robust stability analysis and Llewellyn's criterion are numerically evaluated and compared with each other on two common teleoperation control architectures.**

## I. Introduction

Master-slave teleoperation systems can be modeled as two-port networks coupled to operator and environment one-port networks. The dynamics of operator and environment are usually subject to uncertainty, which results in a compromise between stability and performance, especially in the presence of delay in communication channel [2], [3]. Environments are often unknown and go through drastic changes from free motion to hard contact [4] or from soft tissue to hard bone [5]. Human arm dynamics may not have the wide dynamic range of some environments; however, it is highly variable depending on arm posture, arm muscles activation levels, and fatigue [6], [7]. Therefore, the primary goal of teleoperation control systems design is to guarantee the stability of the interaction between the teleoperation system and the operator and environment, or so-called *coupled stability* [8].

To ensure coupled stability in telerobotic systems, passivity-based robust control methods have been utilized. Passivity of master-slave network (MSN), which is a *sufficient* condition for coupled-stability, has been widely used [9], [10], [11]. This passivity property implies stability regardless of how uncertain the environment and operator impedances are, as long as they are passive; thus, robust stability of MSN. However, passivity of MSN renders a rather conservative robust stability condition. Therefore, the MSN can be active, while the one-port network resulting from the MSN termination with a passive environment be passive. As a result, Llewellyn's absolute stability criterion from circuit theory has been utilized in order to analyze the stability of teleoperation systems and haptic devices coupled with any passive operator and environment [12], [13], [14].

Although, Llewellyn's criterion results in less conservative robust stability condition, the stability analysis still suffers from assumed unrealistic infinite range of operator (human arm) and environment impedances. Thus, researchers have studied the effect of operator and environment impedance on absolute stability. Hashtrudi-Zaad and Salcudean [13] extracted the maximum passive impedances as shunt impedances with the operator and environment one-port networks with infinite range of impedances. They concluded that a more relaxed set of conditions may be found by examining the absolute stability of the new two-port network created by absorbing shunt impedances. Adams and Hannaford [12] utilized the minimum and maximum of the operator arm impedance, whereas Cho and Park [14] used the same approach for both environment and operator impedances. However, this indirect approach in including the effect of bounded environment and operator impedances is the only flexibility of Llewellyn's criterion. If a coupled teleoperation system is shown to be potentially unstable, the Llewellyn's criterion does not provide any clear and direct means of showing for what values of operator and environment impedances the system is stable or for what lower and upper bounds on the environment or operator passive impedances the system is absolutely stable.

Edwards and Sinsky reported a novel robust stability analysis technique for microwave systems [1]. The methodology is based on scattering theory and wave parameters. In this paper, we introduce and develop the robust stability technique in [1] for teleoperation and tailor the methodology for such applications. We further use the technique to derive bounds on the operator and/or environment impedances for stability analysis of potentially unstable systems. Finally, we introduce a new measure of robust stability to obtain the least conservative stability condition. The new methodology provides mathematical and visual aids i) to analyze the stability of a teleoperator when connected to any unknown environment or operator with known bounds, ii) to determine the bounds on environment and/or operator impedance that guarantee coupled stability, iii) to design stable teleoperation systems when such bounds on environment/operator are known, and iv) to analyze the stability of teleoperation systems, even when the environment or operator impedance

This work was supported in part by PRECARN, Ontario Centres of Excellence (OCE), Natural Sciences and Research Engineering Council of Canada (NSERC), Industrial Research Assistance Program (IRAP) and Quanser Consulting Inc.

The authors are with the Department of Electrical and Computer Engineering, Queen's University, Kingston, ON K7L 3N6, Canada. amir.haddadi@ece.queensu.ca, khz@post.queensu.ca

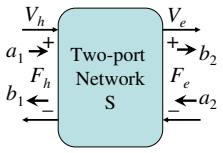


Fig. 1. A typical two-port system.

is active. The strength of the new analysis and design tool is shown through two benchmark examples.

## II. Scattering Operator

Linear two-port networks are characterized by a number of equivalent parameters, such as *impedance* , *admittance hybrid*, or *scattering* matrices [15]. The interaction between different parts of the physical system is fundamentally bilateral and can be shown by efforts ($F_i$) and flows ($V_i$), where $i$ can be $h$ or $e$ denoting the operator hand or environment for teleoperation systems, as shown in Figure 1. The set of scattering variables used in the scattering matrix are *inwave* or *incident wave* $\overrightarrow{w} = [a_1 \ a_2]^T$ and *outwave* or *reflected wave* $\overleftarrow{w} = [b_1 \ b_2]^T$, with the traveling waves $a_1, a_2, b_1$ and $b_2$ defined as:

$$a_1 = \frac{F_h + bV_h}{2\sqrt{b}}, \quad a_2 = \frac{F_e - bV_e}{2\sqrt{b}} \tag{1}$$

$$b_1 = \frac{F_h - bV_h}{2\sqrt{b}}, \quad b_2 = \frac{F_e + bV_e}{2\sqrt{b}} \tag{2}$$

where $b > 0$ is called the characteristic wave impedance. The relation between incident wave and reflected wave is governed by the scattering relation:

$$\overleftarrow{w} = \begin{pmatrix} b_1 \\ b_2 \end{pmatrix} = \begin{pmatrix} S_{11} & S_{12} \\ S_{21} & S_{22} \end{pmatrix} \begin{pmatrix} a_1 \\ a_2 \end{pmatrix} = S\overrightarrow{w} \tag{3}$$

where $S$ is the scattering matrix and its elements are called *scattering parameters* or *S-parameters* [15].

## III. Stability Criterion

A very common method for the stability analysis of circuits and systems uses the equivalent impedance from a driving point of a network in a complicated circuit or system [15]. Consider the block diagram of a teleoperation system as shown in Figure 2, where $F_h^*$ is the exogenous input, $Z_h$ and $Z_e$ are the linear-time-invariant (LTI) impedance models of the operator and environment dynamics, and $Z_{in} := \frac{F_h}{V_h}$ and $Z_{out} := \frac{F_e}{V_e}|_{F_h^*=0}$ are the transmitted impedances to the operator and environment, respectively.

Figure 3 shows the MSN with its Thevenin equivalent network representation, where the network variables $Z_{in}, Z_{out}$ and $F_{h,th}^*$ are expressed in terms of the network impedance matrix parameters as [15]:

$$F_{h,th}^* = \frac{Z_{21}}{Z_{11} + Z_h} F_h^* \tag{4}$$

$$Z_{out} = Z_{22} - \frac{Z_{12}Z_{21}}{Z_{11} + Z_h} \tag{5}$$

$$Z_{in} = Z_{11} - \frac{Z_{12}Z_{21}}{Z_{22} + Z_e} \tag{6}$$

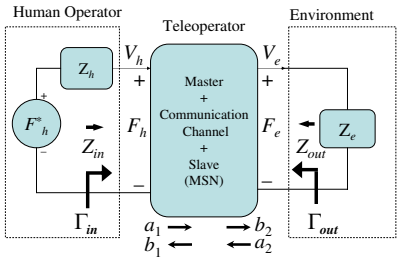


Fig. 2. General block diagram of a teleoperation system.

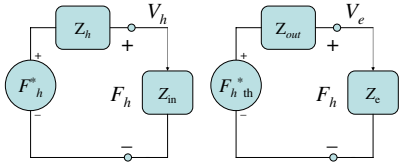


Fig. 3. Impedance representation of the MSN.

### A. Absolute Stability in Scattering Domain

The LTI MSN is *absolutely* or *unconditionally stable* if any passive operator ($Z_h$) or environment ($Z_e$) impedances lead to passive input ($Z_{in}$) or output ($Z_{out}$) impedances; thus, resulting in a stable coupled teleoperation system. This implies that an MSN is absolutely stable if any operator and environment with impedances that lie within the right-half-plane (RHP) of the complex plane will result in input and output impedances that lie in the RHP. However, equations (4)-(6) do not provide an easy way of deriving bounds on the operator and environment impedances for less conservative stability conditions.

As a remedy, scattering parameters, suggested in [1] for communication and microwave systems, are used in this paper. In essence, using the equivalent relations between S-parameters of the teleoperation system, distinct conditions on environment/operator dynamic bounds and teleoperator scattering parameters are achieved. Similar to $Z_{in}$ and $Z_e$ in impedance representation, $\Gamma_{in}$ and $\Gamma_e$ in scattering domain can be defined according to $\Gamma_{in} := \frac{b_1}{a_1}$ and $\Gamma_e := \frac{a_2}{b_2}$. The parameters $\Gamma_{in}$ and $\Gamma_e$ are *reflection coefficients* as seen from the operator and environment, respectively, and they can be written in terms of $Z_e$ and $Z_{in}$ as

$$\Gamma_{in} = \frac{Z_{in} - b}{Z_{in} + b} \quad , \quad \Gamma_e = \frac{Z_e - b}{Z_e + b} \tag{7}$$

Using (6) and the relations between impedance and scattering parameters [15], we obtain:

$$\Gamma_{in} = S_{11} + \frac{S_{12}S_{21}\Gamma_e}{1 - S_{22}\Gamma_e}. \tag{8}$$

Writing similar equations using the reflection coefficient of the operator $\Gamma_h := \frac{a_1}{b_1}|_{F_h^*=0}$ and environment as seen from the environment side $\Gamma_{out} := \frac{b_2}{a_2}|_{F_h^*=0}$, yields:

$$\Gamma_{out} = S_{22} + \frac{S_{12}S_{21}\Gamma_h}{1 - S_{11}\Gamma_h} \tag{9}$$

The advantage of defining reflection coefficients is that the passivity condition from the entire RHP in the Cartesian complex plane reduces to a unit circle, meaning that $|\Gamma_p| < 1$ is equivalent to $Re(Z_p) > 0$ for any $p \equiv e, h, in, out$:

*Proof:* Suppose $\Gamma_p = \frac{Z_p - b}{Z_p + b} := \alpha + \beta j$. Therefore, $Re(Z_p) = -\frac{b(\alpha^2+\beta^2-1)}{(\alpha-1)^2+\beta^2}$. Since $b > 0$, if we require $Re(Z_p) > 0$, then condition $\alpha^2 + \beta^2 < 1$ must hold; thus, $|\Gamma_p| < 1$. ■

Using the above passivity condition for reflection coefficients, absolute stability can be expressed in terms of scattering parameters as: A two-port network is absolutely or unconditionally stable if for any environment and operator dynamics satisfying the passivity conditions $|\Gamma_e| < 1$ and $|\Gamma_h| < 1$, the input and output reflection coefficients satisfy $|\Gamma_{in}| < 1$ and $|\Gamma_{out}| < 1$ [1]; otherwise, the system is called *potentially* or *conditionally* unstable.

The question that arises is what happens if the teleoperation system is not absolutely stable, meaning that $Z_{in}$ is not passive for all passive environment impedances? Can we determine stabilizing bounds on $Z_e$ or $Z_h$ within which the stability of the teleoperation system is guaranteed? To this end, in this paper, we define the new concept of *bounded impedance absolute stability (BIAS)*, which refers to guaranteed system stability as long as environment or operator impedance is limited within the bounds. When the impedance violates these bounds, the system is potentially unstable, meaning that the stability of the teleoperation system in that region is not guaranteed.

We define *environment stability region* as the set of all $\Gamma_e$ that result in passive $\Gamma_e$, *i.e.* $|\Gamma_{in}| < 1$, and *operator stability region* as the set of all $\Gamma_h$ that result in passive $\Gamma_{out}$, *i.e.* $|\Gamma_{out}| < 1$. Therefore, the environment/operator stability region may contain both active and passive environment/operator impedances. In the case of absolutely stable MSN, the environment or operator stability regions contain the passivity unit circles $|\Gamma_e| < 1$ or $|\Gamma_h| < 1$. However, in potentially unstable networks, only portions of the environment or operator passivity unit circles lie within the stability regions in the $\Gamma_h$ or $\Gamma_e$ plane. This overlap between the two regions determines bounds on environment or operator passive impedance within which the entire system is stable.

To graphically visualize the absolute stability, potential stability and BIAS, the environment and operator stability regions should be expressed in terms of $\Gamma_e$ and $\Gamma_h$ and drawn in $\Gamma_e$ and $\Gamma_h$ planes. To this end, the following notions from Edwards and Sinsky [1] are utilized

$$\begin{aligned} r_h &= \frac{|S_{12}S_{21}|}{|D_1|} \quad , \quad c_h = \frac{C_1^*}{D_1} \\ r_e &= \frac{|S_{12}S_{21}|}{|D_2|} \quad , \quad c_e = \frac{C_2^*}{D_2} \\ C_1 &= S_{11} - \Delta S_{22}^* \quad , \quad D_1 = |S_{11}|^2 - |\Delta|^2 \\ C_2 &= S_{22} - \Delta S_{11}^* \quad , \quad D_2 = |S_{22}|^2 - |\Delta|^2 \\ \Delta &= \det(S) = S_{11}S_{22} - S_{12}S_{21} \end{aligned} \tag{10}$$

where the asterisk superscript denotes the complex conjugate operator. After some mathematical operations [1], the environment and operator stability regions can be expressed in terms of $\Gamma_e$ and $\Gamma_h$ and the above parameters as

$$1 - |\Gamma_{out}|^2 > 0 \Leftrightarrow (|\Gamma_h - c_h|^2 - r_h^2)D_1 > 0 \tag{11}$$

$$1 - |\Gamma_{in}|^2 > 0 \Leftrightarrow (|\Gamma_e - c_e|^2 - r_e^2)D_2 > 0 \tag{12}$$

The parameter pairs $(c_h\,,\, r_h)$ and $(c_e\,,\, r_e)$ determine the centers and radii of the operator and environment stability region circles, respectively. Depending on the sign of $D_1$ and $D_2$, operator and environment stability regions fall *outside* (for positive $D_i$) or *inside* (for negative $D_i$) of the stability circles, that is

***Operator Stability Region in*** $\Gamma_h$ ***plane:***

$$|\Gamma_h - c_h| > r_h, \quad if\ D_1 > 0 \tag{13}$$

$$|\Gamma_h - c_h| < r_h, \quad if\ D_1 < 0 \tag{14}$$

***Environment Stability Region in*** $\Gamma_e$ ***plane:***

$$|\Gamma_e - c_e| > r_e, \quad if\ D_2 > 0 \tag{15}$$

$$|\Gamma_e - c_e| < r_e, \quad if\ D_2 < 0 \tag{16}$$

Next, absolute stability and potential instability are described in the environment plane $\Gamma_e$ [1]. In Section IV, we will extend these arguments for BIAS to determine bounds on environment impedance for guaranteed stability. The same argument can be made in the operator plane $\Gamma_h$.

As shown in Figure 4, in order to have absolute stability, the environment stability region must contain the *environment passivity unit circle* $|\Gamma_e| = 1$ in the $\Gamma_e$ plane in its entirety, or alternatively the operator stability region must contain the *operator passivity unit circle* $|\Gamma_h| = 1$ in the $\Gamma_h$ plane in its entirety. If $D_2 > 0$, the environment stability region is outside the *environment stability circle* $|\Gamma_e - c_e| = r_e$ with center $c_e$ and radius $r_e$. Therefore for absolute stability, the environment stability circle and environment unit circle must not overlap. Geometrically, the distance between the plane center $O$ and point $A$ in the figure is $(OA) = |c_e| - r_e$. The non-overlapping condition of the circles requires that $(OA) > 1$, or, $|c_e| - r_e > 1$. In a dual manner, if $D_2 < 0$, the environment stability region is inside of the environment stability circle; therefore, the environment passivity unit-circle must lie within the environment stability circle. This requires that $(OA) = r_e - |c_e| > 1$, as shown in Figure 4. The same analysis can be performed for the operator side ($e \rightarrow h$). The above two stability conditions for environment can be combined into $sign(D_2)(|c_e| - r_e) > 1$. Geometrically, $\mu_2 = sign(D_2)(|c_e| - r_e)$ represents the distance $(OA)$ and was first introduced by Edwards and Sinsky [1]. Thus, the condition for the absolute stability of the input is equivalent to $\mu_2 > 1$ or alternatively $\mu_1 = sign(D_1)(|c_h| - r_h) > 1$.

If the absolute stability condition is not satisfied, that is $\mu_2 < 1$, then only the portion of the environment unit circle that lies within the environment stability region will guarantee stability. Figure 5 illustrates such a potentially unstable case, in which the environment unit circle is partially

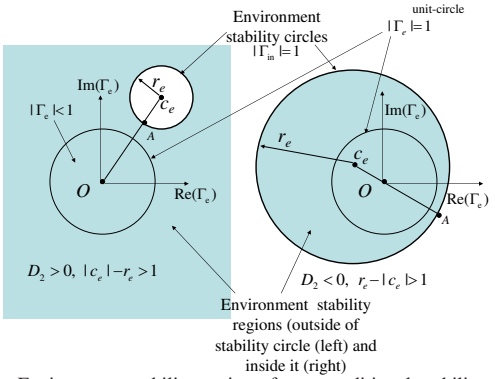


Fig. 4. Environment stability regions for unconditional stability. In this case, environment stability region ($|\Gamma_{in}| < 1$) contains the environment passivity unit circle ($|\Gamma_e| < 1$). The blank areas inside the environment stability circle (left subfigure) and outside the environment stability circle (right subfigure) are potentially unstable regions.

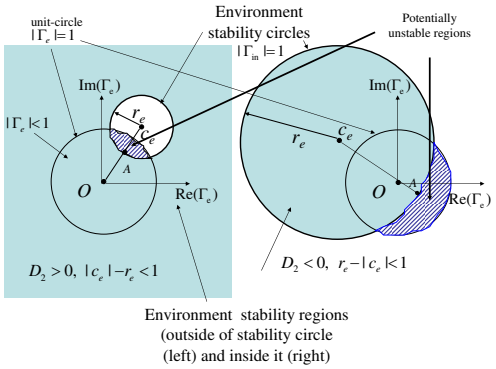


Fig. 5. Environment stability region in the potentially unstable case. The portion of the environment unit-circle that does not lie within the environment stability region corresponds to that region of $Z_{in}$ which makes the system potentially unstable.

overlapping with the environment stability circle. The portion of the unit circle that does not lie within the stability region corresponds to that region of $Z_e$ which makes the system potentially unstable. Therefore, this method demonstrates significant flexibility compared to Llwellyn's method, as we still can achieve stability for some range of impedances (*i.e.* BIAS) if the system is potentially unstable. Similar analysis can be performed for the operator side, while the environment is considered to be passive and some bounds on the operator impedance are known. In fact, this method has the advantages of the methods that consider environment and operator impedances in stability analysis, such as Nyquist, small gain, etc. and the advantages of the methods that consider only the MSN and not the dynamics of environment and operator, such as MSN passivity or Llewellyn's.

It is important to note that if the environment/operator impedance bounds are known, these bounds can be mapped into the scattering domain using $\Gamma_e = \frac{Z_e - b}{Z_e + b}$ or $\Gamma_h = \frac{Z_h - b}{Z_h + b}$. The mapped bounds instead of the unit circles will be utilized in the stability analysis, resulting in less conservative stability conditions. Thus, in potentially unstable cases, in order to analyze the stability of teleoperation systems with bounds on environment/operator impedances, it is required to map $Z_e(Z_h)$ to $\Gamma_e(\Gamma_h)$ plane. Section IV will provide a complete analysis of mapping a group of impedances with LTI mass-damper-spring models.

***Remark:*** In addition to robust stability analysis, another important application of the above approach, *i.e.* (10), (13)-(16), is in the design of teleoperation control systems for guaranteed stability. As the stability circle parameter pairs ($c_h$ , $r_h$) and ($c_e$ , $r_e$) depend on the MSN dynamics, the MSN bilateral control architecture and its control parameters can be chosen to move the stability circle in a way to avoid the unit circles for $D_i > 0$ or to contain the unit circles for $D_i < 0$.

## IV. Mapping $Z_e$ ($Z_h$) Bounds on $\Gamma_e$ ($\Gamma_h$) Plane

As discussed before, in the case of potential instability we need to map the environment(operator) impedance into the $\Gamma_e(\Gamma_h)$ plane in order to analyze the stability of the coupled system. In this section, rectangular regions of $Z_e(j\omega)$ will be transformed into circular regions of $\Gamma_e(j\omega)$ in the complex plane. Furthermore, for the first time, the concept of *Smith Chart* from microwave analysis and antenna design [16] will be introduced into teleoperation to map any arbitrary region of complex plane that $Z_e(j\omega)$ might lie within, into the $\Gamma_e$ plane. The same approach can be utilized for operator hand impedance. Therefore, this helps us prove the stability of potentially unstable systems, while *a priori* knowledge of the environment/operator impedance is available.

### A. Impedance Circles

In this section, we plan to map the impedance of an LTI environment, that is $Z_e(j\omega) = B_e + jX_e(j\omega)$ to its corresponding reflection parameter $\Gamma_e = \Gamma_{er} + j\Gamma_{ei}$ in the scattering domain. Assuming $b = 1$ [1] and using (7), the $Z_e$ can be expressed in terms of $\Gamma_e$ as

$$Z_e = B_e + jX_e = \frac{1+\Gamma_e}{1-\Gamma_e} = \frac{1+\Gamma_{er}+j\Gamma_{ei}}{1-\Gamma_{er}-j\Gamma_{ei}} \tag{17}$$

Extracting the real and imaginary parts, yields

$$B_e = \frac{1-\Gamma_{er}^2-\Gamma_{ei}^2}{(1-\Gamma_{er})^2+\Gamma_{ei}^2} \tag{18}$$

$$X_e = \frac{2\Gamma_{ei}}{(1-\Gamma_{er})^2+\Gamma_{ei}^2} \tag{19}$$

After rewriting (18) to the following equation as shown in [16]

$$(\Gamma_{er} - \frac{B_e}{B_e+1})^2 + \Gamma_{ei}^2 = (\frac{1}{B_e+1})^2 \tag{20}$$

one notices that any vertical line in $Z_e$ representing environment equivalent damping is mapped to an "impedance

[1] If $b \neq 1$, we have to divide both numerator and denominator by $b$.

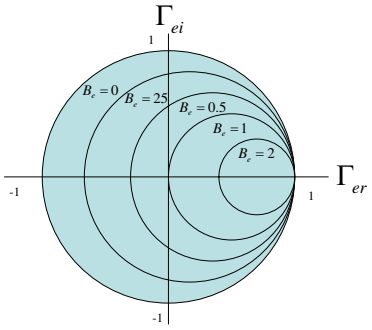


Fig. 6. Impedance circles for different damping values.

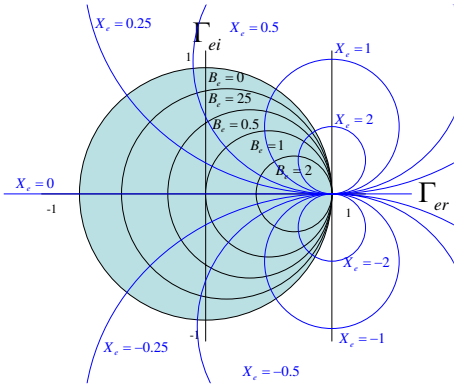


Fig. 7. Smith circles employed to map impedance bounds from impedance domain to scattering domain.

circle" in the $\Gamma_e$ plane. As shown in Figure 6, the radii and the location of the centers of impedance circles only depend on damping $B_e$. By increasing $B_e$ from zero to $\infty$ (large values), the impedance circles centers move horizontally from the point $(0, 0)$ to the point $(1, 0)$, whereas the radius decreases from 1 to 0, respectively. Therefore, the larger the minimum environment damping, the smaller the environment stability region is required to include the stability circles. This intuitive result that will further be explored through some examples in the next section, also points at an important notion that only bounds on damping is enough to determine whether the environment impedances within the bounds (ensemble of circles) are inside the environment stability region or not. If they are, then they do not intersect with the environment stability region; thus, robust stability is guaranteed while the system is potentially unstable. If these circles intersect with the environment stability circle, no conclusion on stability can be drawn since the intersection might happen at two different frequencies for impedance and stability circles. In such case, a new frequency-dependent stability parameter ($\gamma_e(j\omega)$) is needed, which will be proposed in the next section. The above argument can be made for operator arm damping, as well as the geometrical relation between operator impedance circles and operator stability region. It is very interesting to note that since the damping parameter of the human arm impedance normally changes over a smaller range compared to the arm stiffness [6], a less conservative controller, designed for the variations of the arm impedance, is expected to maintain the stability of the system.

As mentioned above, an LTI impedance $Z_e(j\omega) = B_e + jX_e(j\omega)$ with constant damping which is a line in impedance domain maps into a circle in scattering domain. As operational frequency changes, $X_e(j\omega)$ changes and impedance moves up and down on the line. Two questions that rises are i) how the reflection coefficient $\Gamma_e$ moves on impedance circles for various frequencies, and ii) how this motion is affected by the environment equivalent mass $M_e$ and stiffness $K_e$ components in $X_e = M_e\omega - K_e/\omega$. To answer these questions, equation (19) is reformatted as

$$(\Gamma_{er} - 1)^2 + (\Gamma_{ei} - \frac{1}{X_e})^2 = (\frac{1}{X_e})^2. \tag{21}$$

The loci of $X_e$ in the $\Gamma_e$ plane are circles with center $(1, 1/X_e)$ and radius $1/X_e$, as shown in Figure 7. The intersection of these circles with impedance circles show the actual reflection coefficient at every single frequency. Therefore, changing frequency, mass or stiffness will change the loci of the centers of these vertical circles as well as their radii. If $M_e = 0$ (also known as capacitive impedance) vertical circles exist only in the bottom half of the plane and thus only bottom half of impedance circles are considered for environment impedance bound. In a dual manner, if environment is dominated by mass and damping properties, only the upper half circles will exist. Figure 7 shows the two sets of circles together. These circles, when drawn in the unit circle, are known as *smith circles*, and can be found in Smith Charts [16]. Smith Charts were developed before the advent of the modern computers for the analysis of stability of transmission lines and matching circuits, and it has primarily been used in microwave and RF systems. This is the first time that the Smith Chart concept is utilized for mapping the environment/operator impedance into impedance circles to analyze the stability of potentially unstable teleoperation systems.

## V. Geometric Implications of the New Method versus Llewellyn's Criterion

In this section, the robustness stability of two teleoperation control architectures are numerically analyzed using the new method and Llewellyn's absolute stability criterion. The stability conditions obtained using the two methods are compared.

### A. Four-channel Bilateral Control Architecture

Consider the general block diagram of a four-channel bilateral teleoperation control system as shown in Figure 8, where $Z_m = 0.7s$ and $Z_s = 0.5s$ are master and slave mass models, $C_m = 29.4 + 630/s$ and $C_s = 1300 + 25000/s$

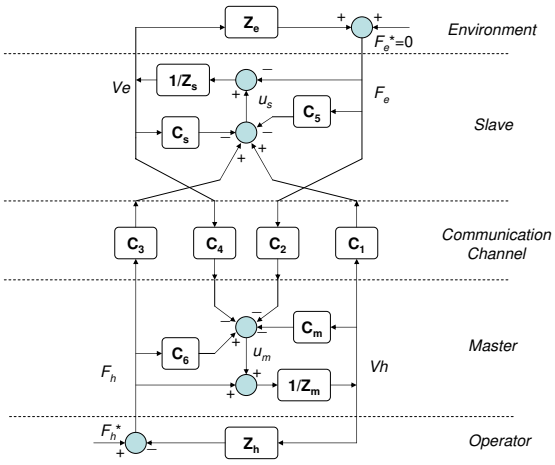


Fig. 8. Block diagram of a four-channel bilateral control system.

represent master and slave position controllers, $C_1, ..., C_4$, are remote compensators, and $C_5$ and $C_6$ are master and slave local force feedback controllers.

Transparency Optimized Control (TOC): We consider that $C_1, ..., C_6$ are chosen according to the transparency-optimized control (TOC) law $C_1 = Z_s + C_s, C_2 = 1 + C_6 = 1, C_3 = 1 + C_5 = 1$ and $C_4 = -(Z_m + C_m)$ for perfect transparency in the case of negligible delays [2], [13]. As shown in [13] and illustrated in Figure 9(b), the TOC system is marginally absolutely stable as the stability parameter of Llewellyn's criterion is unity for all frequencies, that is $\eta = 1, \ \forall \omega > 0$.

In order to visualize the analysis results of the new method, we have to calculate $r_e(\omega)$ and $c_e(\omega)$ or alternatively $r_h(\omega)$ and $c_h(\omega)$. This means that the loci and radii of the stability circles at every frequency should be calculated and plotted. We note from [9] that for $b = 1$, $S = diag(1, -1)[H - I][H + I]^{-1}$ and also that for perfect transparency, $S_{ideal} = \begin{pmatrix} 0 & 1 \\ 1 & 0 \end{pmatrix}$ must hold for all frequencies, where $I$ is a $2 \times 2$ identity matrix. Substituting the components of the ideal S-matrix in (10), we obtain $c_e = c_h = 0$ and $r_e = r_h = 1$ for all frequencies. This means that both operator and environment stability circles are tangent to the operator and environment unit circles at all frequencies. Since $D_1 = D_2 = -1 < 0$ the environment and operator impedances must lie inside the stability circles implying absolute stability. Figure 9 compares Llewellyn's absolute stability parameter with the new geometrical approach for the transparency-optimized four-channel control architecture.

TOC without acceleration: Since acceleration is mostly found from double differentiation of the measured position, it is mostly noisy and unreliable. As a result Lawrence in [2] suggested the use of remote position and velocity feedback, *i.e.* $C_1 = C_s$ and $C_4 = -C_m$, for transparency in low-mid range of frequencies. In such case, as shown in Figure 10(b), for $0.001 < \omega < 1000 \ rad/s$, $\eta < 1$ . In fact $\eta < 1$ for all

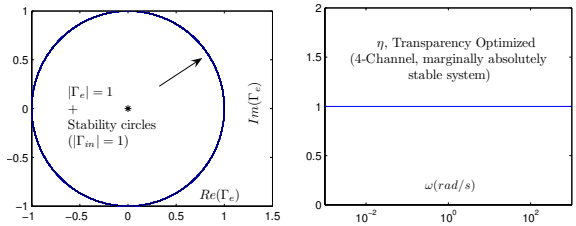


(a) New approach (b) Llewellyn's stability parameter

Fig. 9. Stability analysis of the transparency optimized four-channel teleoperation system.

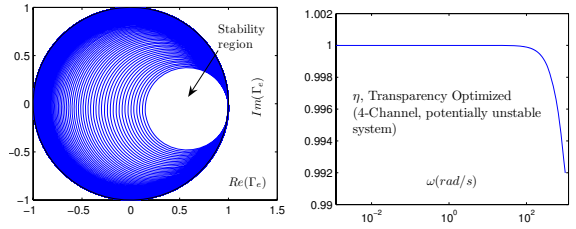


(a) New approach (b) Llewellyn's stability parameter

Fig. 10. Stability analysis of the transparency optimized four-channel teleoperation system (without acceleration feedback).

frequencies; thus, the system is no longer absolutely stable. The Llewellyn's criterion does not provide any clear indication as for what range of environment/operator impedances in a specific range of frequencies the system stability is guaranteed, or whether or not there exist such range of environment/operator impedances. However, the new method is capable of addressing the above questions.

Figure 10(a) shows the environment stability circle for various frequencies, with the outer unit circle for $\omega = 0.001 \, rad/s$ and the inner circle for $\omega = 1000 \, rad/s$. For $\omega > 1000$, the blank circular area is filled. In this case, $-1 < D_2 < 0$ and since the stability circles for all frequencies are inside the environment unit circle, there are some passive environment impedances that cause instability in the system. This instability region is the dark area inside the environment unit circle. If we decrease the frequency range, the inner stability region grows, and hence the instability region shrinks, and vice-versa.

*Stability Analysis with Environment Impedance Bounds*: As discussed in this section, the main advantage of the new robust stability analysis tool is that it incorporates the effect of environment in the stability analysis, which makes it very powerful for in depth analysis of potentially unstable cases such as TOC without acceleration. Figure 11 shows the environment unit circle, the stability circle for the maximum operational frequency $\omega = 1000 \ rad/s$ and the mapped environment impedance $Z_e = B_e + K_e/s$ on the $\Gamma_e$ plane for $B_e > 1.45 \, Nm/s$. Since the mapped $Z_e$ for the above range of damping lies within the stability circle, the above damper-spring environment guarantees system stability with any passive operator for frequency range $0 < \omega < 1000 \ rad/s$, which is larger than the maximum

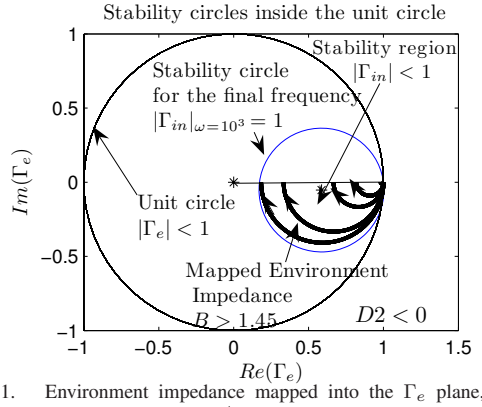


Fig. 11. Environment impedance mapped into the $\Gamma_e$ plane, plus the stability circle for $\omega = 1000\,rad/s$ in TOC without acceleration feedback.

bandwidth required from any teleoperation system. In fact, comparing Figure 11 with impedance circles in Figure 6 reveals that this system is stable for a large group of mass-damper-spring environments with any mass and spring as long as the environment damping is confined to $B > 1.45\,Nm/s$. ***Remark:*** It is important to note that by increasing the system required bandwidth or maximum operational frequency $\omega$, the smallest stability circle shrinks, and as a result the minimum $B_e$ required for guaranteed stability increases, and vice-versa.

### *B. Force-Position Bilateral Control Architecture*

In the second example, consider a force-position (FP) control architecture obtained by setting $C_3 = C_4 = 0$ in the four-channel TOC law. Figure 12(b) shows the Llewellyn's absolute stability parameter, which only tells that the system is potentially unstable ($\eta(\omega) < 1$), for $\omega > 935\,rad/s$. Figure 12(a) shows the environment unit circle, the stability circles for various frequencies, and the mapping of $Z_e = 10 + 0.7/s$ into the $\Gamma_e$ plane (impedance circle). For frequency range $\omega < 935\,rad/s$ the stability circles are to the right of the environment unit circle, as a result the MSN is absolutely stable. For $\omega > 935\,rad/s$ the stability circles cross the unit circle and the MSN is potentially unstable, as predicted by Llewellyn's criterion. As one can see, the half-circle mapped environment $Z_e = 10 + 0.7/s$ intersects with the stability circles for $\omega > 935\,rad/s$. However, no conclusion with regard to the stability or instability of the entire system for all passive operators can be drawn, unless we examine the frequencies of intersections. In order to see if the intersection happens at the same frequency, a new stability measure is proposed in this paper.

The new stability parameter should include frequency $\omega$ and $D_2$ to make the analysis independent of the frequency and the sign of $D_2$. Therefore, considering (11) and (12), we propose

$$\gamma_e(\omega) = (|\Gamma_e(\omega) - c_e(\omega)|^2 - r_e^2(\omega))D_2. \qquad (22)$$

Therefore, if $\gamma_e > 0$, the stability of the system is guaranteed as long as the operator impedance is passive. Figure 13 shows $\gamma_e$ for the FP bilateral control system for our specific

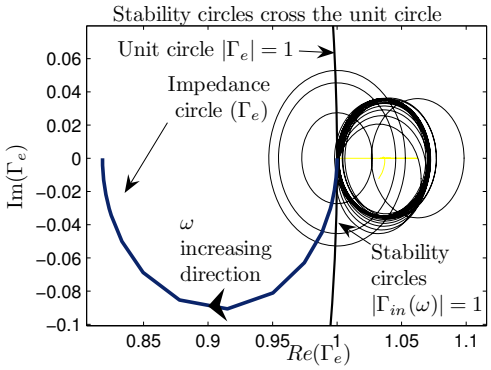


(a) New approach

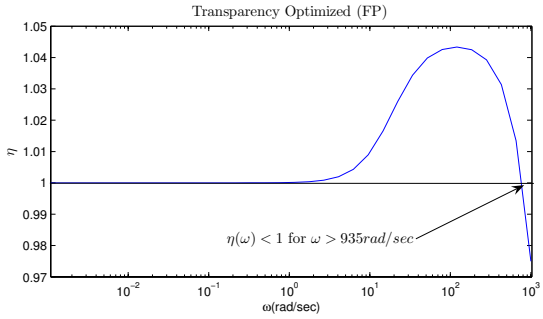


(b) Llewellyn's stability parameter

Fig. 12. Stability analysis of the transparency optimized teleoperation system (FP architecture-without acceleration feedback terms).

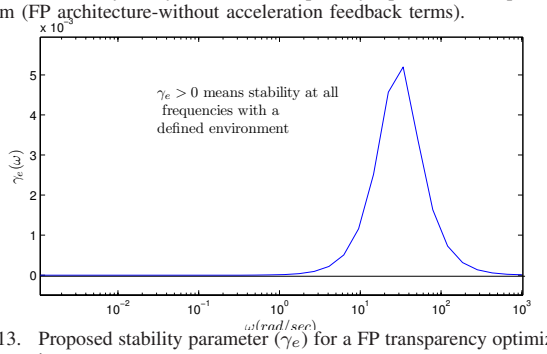


Fig. 13. Proposed stability parameter ($\gamma_e$) for a FP transparency optimized teleoperation system.

impedance. The figure reveals that the entire system is stable with $Z_e = 10 + 0.7/s$ for any passive operator impedance for the whole considered frequency range.

***Remark:*** It is important to note that the intersection of stability circles and mapped impedances in the four-channel architecture happens at the same frequency ($\omega = 1000$ for $B = 1.45$). This is due to the fact that $\Gamma_e(\omega)$ is moving from point $(1, 0)$ to $(0, 0)$ on the impedance circle as the frequency increases. Thus, the reflection coefficient on the mapped impedances approach the stability circles as shown in Figure 11. However, in the FP architecture, as shown in Figure 12(a), as frequency grows the stability circles and $\Gamma_e(\omega)$ on the mapped impedance half-circle move in the same direction.

If the bounds on the environment impedance are known (instead of actual values), then the stability parameter has to

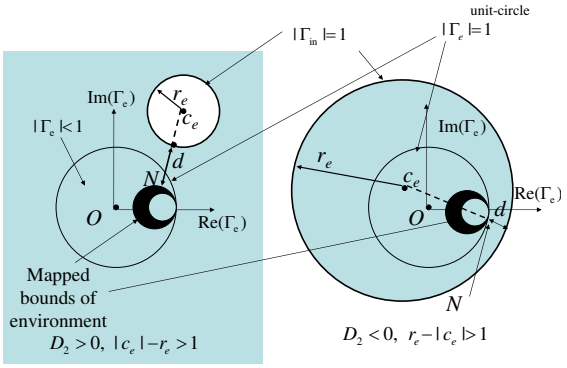


Fig. 14. Proposed stability parameter ($\bar{\gamma}_e$) when bounds on the environment impedance are known.

consider these bounds. Thus, at every frequency there is a region of possible environments. Figure 14 shows this region which is mapped into the $\Gamma_e$ plane in black color. At every frequency the *closest point* of this region to the instability region is shown by $N$ in Figure 14. The distance ($d$) between $N$ and the stability circle, can be determined by the following equation:

$$d = \begin{cases} Min(|\Gamma_e(\omega) - c_e(\omega)|) - |r_e| & D_2 > 0 \\ -[Max(|\Gamma_e(\omega) - c_e(\omega)|) - |r_e|] & D_2 < 0 \end{cases}$$

where the negative sign for the second equation is to prevent negative sign for the distance, when the environment unit circle is inside the stability circle. If one of the above distances becomes negative, a portion of the environment bounds, lies inside the potentially unstable region. In this case, the absolute values in the above equation can equivalently be replaced by power 2. Therefore, the following stability parameter is defined

$$\overline{\gamma}_e(\omega) = \begin{cases} Min(|\Gamma_e(\omega) - c_e(\omega)|)^2 - r_e^2(\omega))D_2(\omega) & D_2(\omega) > 0 \\ Max(|\Gamma_e(\omega) - c_e(\omega)|)^2 - r_e^2(\omega))D_2(\omega) & D_2(\omega) < 0 \end{cases}$$

The above analysis is performed without considering any bounds on the operator impedance. Similar stability parameter can be defined and used for the operator impedance with known bounds, while the environment is passive.

## VI. Conclusions and Future Works

In this paper, a powerful robust stability analysis and design tool from microwave and communication systems has been introduced and developed for teleoperation systems. The new technique incorporates bounds on environment or operator impedance for potentially unstable systems so as to reach a less conservative coupled stability condition and thus a better trade off between stability and performance. The analysis is performed using visual approach or a newly proposed stability parameter, which tends to maximize the derivation of the bounds. Using the new method, we can determine the environment/operator impedance regions in which the teleoperation system is stable. Equivalently, if bounds on environment impedance are known, the coupled stability can be analyzed. Moreover, the new technique can be used when the environment or operator system is active.

In case of environments with LTI mass-damper-spring models, a quick analysis of stability can be performed when only the bounds on the environment damping are known, regardless of the environment mass and spring. The proposed technique and Llewellyn's criterion are both numerically evaluated on a four-channel and a force-position two channel teleopertaion systems. The new method has been utilized to obtain bounds on environment damping for coupled stability for reasonably large range of operational frequencies. The proposed stability metric, provided a wider range of stable environment impedance for the F-P architecture. The design of control systems with the aim of controlling stability circles or equivalently stability parameter is considered for future work. The application of this method in the stability analysis of potentially unstable systems when communication channel time delay is significant is also considered for future work.

## References


[1] M. L. Edwards and J. H. Sinsky, "A new criterion for linear 2-port stability using a single geometrically derived parameter," *IEEE Trans. on Microwave Theory and Techniques*, vol. 40, no. 12, pp. 2303–2311, Dec. 1992.

[2] D. A. Lawrence, "Stability and transparency in bilateral teleoperation," *IEEE Trans. on Robot. and Auto.*, vol. 9, no. 5, pp. 624–637, Oct. 1993.

[3] J. Yan and S. E. Salcudean, "Teleoperation controller design using $h_\infty$-optimization with application to motion-scaling," *IEEE Trans. on Cont. Sys. Tech.*, vol. 4, no. 3, pp. 244–258, May 1996.

[4] L. F. Penin, K. Matsumoto, and S. Wakabayashi, "Force reflection for ground control of space robots," *IEEE Robot. & Auto. Magazine*, vol. 7, no. 4, pp. 50–63, Dec. 2000.

[5] R. H. Taylor and D. Stoianovici, "Medical robotics in computer-integrated surgery," *IEEE Trans. on Robot. and Auto.*, vol. 19, no. 5, pp. 765–781, Oct. 2003.

[6] N. Hogan, "Controlling impedance at the man/machine interface," in *Proceedings of IEEE Int. Conf. on Robot. and Auto.*, Scottsdale, AZ, USA, May 1989, pp. 1626–1631.

[7] F. Mobasser and K. Hashtrudi-Zaad, "A method for online estimation of human arm dynamics," in *Proc. IEEE Int. Conf. of Eng. in Medicine and Biology Society*, 2006, pp. 2412–2416.

[8] E. Colgate and N. Hogan, "An analysis of contact instability in terms of passive physical equivalents," in *Proc. IEEE Int. Conf. on Robot. and Auto.*, Scottsdale, AZ, USA, May 1989, pp. 404–409.

[9] R. J. Anderson and M. W. Spong, "Bilateral control of teleoperators with time delay," *IEEE Trans. on Auto. Cont.*, vol. 34, no. 5, pp. 494–501, May 1989.

[10] D. Lee and M. W. Spong, "Passive bilateral teleoperation with constant time delay," *IEEE Trans. on Robot.*, vol. 22, no. 2, pp. 269–281, Apr. 2006.

[11] J.-H. Ryu, D.-S. Kwon, and B. Hannaford, "Stable teleoperation with time-domain passivity control," *IEEE Trans. on Robot. and Auto.*, vol. 20, no. 2, pp. 365–373, Apr. 2004.

[12] R. J. Adams and B. Hannaford, "Control law design for haptic interfaces to virtual reality," *IEEE Trans. on Trans. Cont. Sys. Tech.*, vol. 10, no. 1, pp. 3–13, Jan. 2002.

[13] K. Hashtrudi-Zaad and S. E. Salcudean, "Analysis of control architectures for teleoperation systems with impedance/admittance master and slave manipulators," *Int. J. Robot. Res.*, vol. 20, no. 6, pp. 419 – 445, 2001.

[14] H. Cho and J. Park, "Impedance control with variable damping for bilateral teleoperation under time delay," *JSME Int. J. Series C*, vol. 48, no. 4, pp. 695–703, 2005.

[15] S. S. Haykin, *Active Network Theory*. Addison-Wesley Publishing Co., 1970.

[16] D. M. Pozar, *Microwave Engineering*, 3rd ed. John Wiley and Sons, Inc., 2005.